E-ISSN 2656-8039
INTERNATIONAL JOURNAL OF ENVIRONMENT, ENGINEERING & EDUCATION
www.ijeedu.com
Vol. 3, No. 1, 2021

Research Article

Estimating and Monitoring the Land Surface Temperature (LST) Using Landsat OLI 8 TIRS

Muhammad Rais Abidin[1], Rahmi Nur[2], Erikha Maurizka Mayzarah[3], Ramli Umar[1]

[1]Department of Geography, Universitas Negeri Makassar, Makassar 90222, Indonesia
[2]Department of Fisheries, Universitas Sulawesi Barat, Majene 91412, Indonesia
[3]Department of Geological Engineering, Universitas Papua, Manokwari 98314, Indonesia
Contact email: muhraisabidin@unm.ac.id, rahminur1987@gmail.com, e.mayzarah@unipa.ac.id, ramliumar707@yahoo.com

Received: *February 14, 2021;* ***Accepted:*** *March 15, 2021;* ***Published:*** *April 18, 2021*

Abstract: Land Surface Temperature (LST) is average temperature of an element of the exact surface of the Earth calculated from measured radiance which depends on the albedo, the vegetation cover, and the soil moisture. Land Surface Temperature can affect human discomfort, health problem, higher energy bill and further reduce the habitability of urban and sub urban area as Makassar city has been recently undergoing massive urban development. This study tries to monitor and estimate Land Surface Temperature by using Landsat 8 TIRS and the data analyzed by vegetation index, and temperature index in order to derive Land Surface Temperature value. The result shows that the vegetation area declined around 3470 hectares in the last four years while the urban area increased approximately 1509 hectare. In addition, 2015, Makassar, South Sulawesi, Indonesia are experienced the highest temperature at 32 degree Celsius while 2019 shown that the maximum heat reached 29 degree celsius. However, the moderate and high temperature (26 – 29 degree Celsius) in 2019 expand and cover wider area than in 2015 as the area of vegetation declined and built-up area increased significantly.

Keywords: Climate Change, Global Warming, Land Use, Urban Index, Vegetation Indices.

1. Introduction

Global warming has always been a trending topic of conversation for almost all people in the world [1]. It seems that the hot issues related to global warming never run out. Global warming is very concerned by the world because it has a very extraordinary impact on the earth [2]. The temperature of the earth's surface every year has an increasing trend. One of the causes of global warming based on several studies is the Urban Heat Island (UHI) [3]–[6]. UHI is analogous to an "island" which has a hot surface temperature concentrated in an urban area and the temperature will decrease in the surrounding suburban/ rural areas. The time series shows (Figure 1) the combined global land and marine surface temperature record from 1850 to 2020. Last year (2020) was the second warmest on record using our latest analysis, referred to as HadCRUT5 Analysis [7].

According to the EPA (Environmental Protection Agency) in 2005, the Urban Heat Island phenomenon is a major problem in every developing city in the world against global warming. This problem is also supported by the increasing urbanization process in a city which seems to never stop. Urbanization, which is said to be a phenomenon of rural residents moving to urban areas, causes many new buildings and buildings as well as the conversion of open land to built-up land which is needed to support various human activities [8], [9].

Massive infrastructure development in the development of a city often does not care about the balance of the ecosystem and environmental quality [10].

This Article Citation: *M. R. Abidin, R. Nur, E. M. Mayzarah, R. Umar, "Estimating and Monitoring the Land Surface Temperature (LST) Using Landsat OLI 8 TIRS," Int. J. Environ. Eng. Educ., vol. 3, no. 1, pp. 17-24, 2021.*

Uncontrolled land use change in the development of a city changes the microclimate in a city. The air temperature condition in urban areas is higher than the surrounding air temperature due to the development of the city [11], [12]. On hot days, the temperature in the city can be around 3-10 degrees Celsius higher than the surrounding air temperature. Studies related to temperature are very important because temperature greatly affects air quality, affects human health, and affects energy use. Surface temperature in the Urban Heat Island phenomenon is one of the biggest factors causing climate change and global warming. Some of the negative effects of the Urban Heat Island include the deaths of hundreds of people in the summer due to heat waves in urban areas, a reduction in water quality in urban areas due to pollution from excessive heat, and an increase in electricity consumption by 5-6 percent. As a result of the increasing use of electricity, it encourages the increase in the use of fossil fuels which causes global warming.

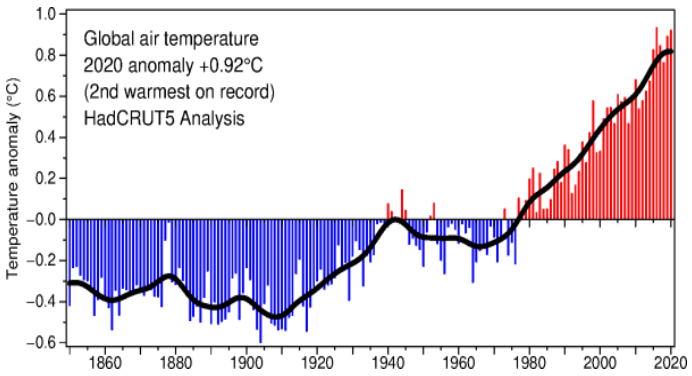

Figure 1. Global Air Temperature

Global warming influences air and temperature with implication for human discomfort, health problem and animal diseases [13]. Heat wave is due to surface energy and water balance which can significantly affects a wide variety of applications such as vegetation monitoring, urban climate, climate change and the hydrological cycle [14], [15]. The combination of green vegetation, water surfaces, exposed soils, impervious underground materials is the very complex feature of the land surface. Impervious varies dramatically between urban and sub urban area which lead to the key contributor of an increase of Land Surface Temperature (LST) [16], [17]. Due to its massive affect, calculating and monitoring transformation in land surface temperature and air temperature play crucial part to asses and forecast the risks such as heat stress and high energy bills. Recently, remote sensing is an important tool for understanding the spatiotemporal Land Use and Land Cover (LULC) related to the basic physical properties in terms of the surface radiance and emissivity data. Since the 1970s, satellite-derived (such as Landsat Thematic Mapper-TM) surface temperature data have been employed for local and regional climate analyses on different area and zone [18], [19]. Like other cities in developing nation, Makassar city has been recently undergoing massive transformation in land use and land cover due to rapid population growth which led to an increase demand of residence, housing, transportation facilities, parking area, educational facilities, shopping mall and governmental building. In addition to massive changes in land use and land cover, it can degrade the protected forest and food chain in mangrove area [20], [21].

Before the Landsat satellite, it was difficult to estimate the Land Surface Temperature (LST) of an area. Generally, it is calculated for a given set of sample points and interpolated into an isotherm to generalize the point data to regional data. Now with the advent of satellites and high-resolution sensors it is possible to estimate LST spatially. This can be calculated in the area recorded by the satellite's thermal infrared sensor. Landsat 8 comes with two different sensors, namely the OLI sensor with nine bands (bands 1-9) and the TIRS sensor with two bands (band 10 and band 11) [22].

The main sensor of Landsat 8 is the Operational Land Imager (OLI) which has a function to collect data on the earth's surface with spatial and spectral resolution specifications that are continuous with previous Landsat data. OLI is designed in a push-broom sensor recording system with four mirror telescopes, better signal to noise performance, and storage in a 12-bit quantification format. OLI records images in the visible wavelength spectrum, near infrared, and middle infrared which has a spatial resolution of 30 meters, as well as panchromatic channels that have a spatial resolution of 15 meters.

Two new spectral channels were added to the OLI sensor, namely a deep-blue channel for the study of marine waters and aerosols and a channel for detecting cirrus clouds. A quality assurance channel has also been added to indicate the presence of terrain shadows, clouds, etc. Thermal Infrared Sensor (TIRS) is the second sensor embedded in Landsat 8. TIRS functions to sense temperature and other applications, such as evapotranspiration modeling to monitor water use in irrigated land [23]. TIRS records images on two thermal infrared channels and is designed to operate for 3 years. The spatial resolution of the TIRS is 100 meters and is registered with the OLI sensor, resulting in radiometric and geometrically calibrated images that are field corrected with a correction level of 1T and stored in the 16-bit system [24].

The fact that Makassar has been experiencing an increase of land surface temperature come from several research such as Land Surface Temperature Makassar and Jakarta stated that the highest temperature at 32 – 35 degree Celsius distributes in the downtown area with high

population density related to residential area, offices, and shopping mall [25], [26]. Meanwhile, the lowest heat at 29 – 31 degree Celsius located mostly in hinterland which dominated by bareness area, woodland, and farmland [27]. The objective of this study is to estimate and monitor the progress of land surface temperature by using the Urban Index (UI) to identify the non-urban and urban area and Normalized Difference Vegetation Index (NDVI) to classify the non-vegetation and vegetation area by employing images taken from Landsat OLI 8 TRS in different time periods. As a result, this research will attempt to identify the correlation between Urban Index (UI) and Normalized Difference Vegetation Index (NDVI) in order to estimate and monitor the progress of land surface temperature from 2015 to 2019 and the distribution of heat wave in Makassar city.

2. Research Methods

2.1. Study Area

This research takes a place in Makassar city (119°24'17'38" East Longitude and 5°8'6'19" South Latitude) which bordered by Maros Regency at the North, Maros Regency at the East, Gowa Regency at the South, and Makassar Strait at the West. Makassar has 14 districts with area of 175, 77 square km [28]. The study area can be seen in the following figure.

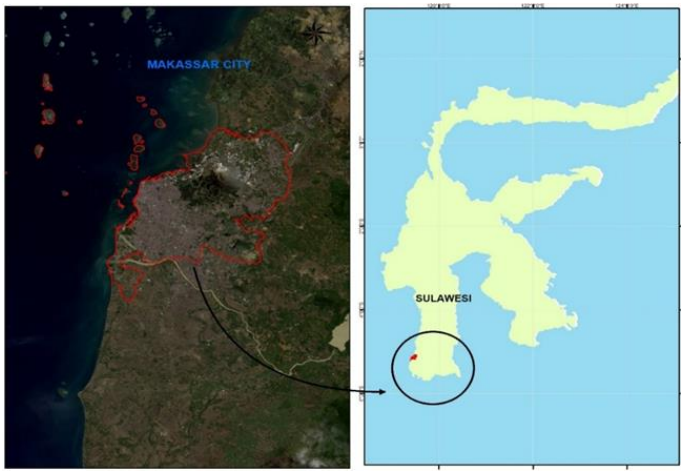

Figure 2. Study Area (Makassar, South Sulawesi, Indonesia)

The data in this research employed is Landsat 8 OLI TIRS satellite images with 30-meter spatial resolution of Makassar (Path = 114, Row = 64) acquired in different time from 27 April 2015 to 13 September 2019. Landsat 8 can record images with various spatial resolutions. Spatial resolution varies from 15-100 meters and is equipped with 11 bands with varying spectral resolutions. Landsat 8 is equipped with two sensor instruments, namely OLI and TIRS. Landsat 8 can collect 400 scene imagery or 150 times more than Landsat 7 in one day of recording.

2.2. Land Surface Temperature (LST)

- Conversion to TOA Radiance

OLI and TIRS band data can be converted to TOA spectral radiance using the radiance rescaling factors provided in the metadata file [13]. The following equation is used to convert OLI and TIRS band to TOA radiance for OLI data as follows:

$$L_\lambda = M_L\, Q_{cal} + A_L \quad (1)$$

L_λ = TOA spectral radiance (Watts/(m2 * srad * μm).
M_L = Band-specific multiplicative rescaling factor from the metadata.
Q_{cal} = Band-specific additive rescaling factor from the metadata.
A_L = Quantized and calibrated standard product pixel values (DN).

- Conversion to TOA Reflectance

OLI band data can also be converted to TOA planetary reflectance using reflectance rescaling coefficients provided in the product metadata file (MTL file) [13]. The following equation is used to convert DN values to TOA reflectance for OLI data as follows:

$$\rho\lambda' = M_\rho\, Q_{cal} + A_\rho \quad (2)$$

$\rho\lambda'$ = TOA planetary reflectance, without correction for solar angle.
M_ρ = Band-specific multiplicative rescaling factor from the metadata
Q_{cal} = Band-specific additive rescaling factor from the metadata
A_ρ = Quantized and calibrated standard product pixel values (DN)

TOA reflectance with a correction for the sun angle is then:

$$\rho\lambda = \frac{\rho\lambda'}{\cos(\theta_{SZ})} = \frac{\rho\lambda'}{\sin(\theta_{SE})} \quad (3)$$

$\rho\lambda$ = TOA planetary reflectance.
θ_{SZ} = Local sun elevation angle. The scene centre sun elevation angle in degrees is provided in the metadata (SUN_ELEVATION)
θ_{SE} = Local solar zenith angle; $\theta_{SZ} = 90° - \theta_{SE}$

- Conversion to Top of Atmosphere Brightness Temperature

TIRS band data can be converted from spectral radiance to top of atmosphere brightness temperature using the thermal constants provided in the metadata file [29]. The following equation is used to convert spectral radiance to

top of atmosphere brightness temperature for OLI data as follows:

$$T = \frac{K_2}{ln\left(\frac{K_1}{L_\lambda} + 1\right)} \quad (4)$$

T = Top of atmosphere brightness temperature (K).
L_λ = TOA spectral radiance (Watts/ (m2 * srad * µm)).
K_1 = Band-specific thermal conversion constant from the metadata.
K_2 = Band-specific thermal conversion constant from the metadata.

- Deriving LSE (Land Surface Temperature)

$P_v = \left(\frac{NDVI - NDVImin}{NDVImax - NDVI\ min}\right)^2$
P_v = TOA spectral radiance (Watts/ (m2 * srad * µm)).
e = $0.004\ Pv + 0.986$

Convert the At-Satellite Brightness Temperature to Land Surface Temperature, using the following equation

$$\frac{BT}{1} + w \times \left(\frac{BT}{p} \times 1n\ (e)\right) \quad (5)$$

BT = At Satellite Temperature
w = Wavelength of emitted radiance (11.5µm)
P = h * c / s ($1.438 * 10^{-2}$ m K)
h = Planck's constant ($6.626 * 10^{-34}$ Js)
s = Boltzmann constant ($1.38 * 10^{-23}$ J/K)
c = Velocity of light ($2.998 * 10^{8}$ m/s)
p = 14380

2.3. Vegetation Indices (VI)

The vegetation indices options include NDVI, EVI, SAVI, and MSAVI. Products are generated at 30-m spatial resolution on a Universal Transverse Mercator (UTM) or Polar Stereographic (PS) mapping grid. The default file format is Geo tiff, but options for delivery in Hierarchical Data Format (HDF) and binary are available through the ESPA Ordering Interface. Processing services can be requested such as projection and spatial sub-setting. Temporal coverage varies depending on the selected sensor, with the exceptions noted in Section 2 Caveats and Constraints [29], [30]. Meanwhile Normalized Difference Vegetation Index (NDVI) is calculated as a ratio between the red (R) and near infrared (NIR) values in traditional fashion that can be seen in equation below.

In Landsat 4

$$NDVI = \frac{Band\ 4\ -\ Band\ 3}{Band\ 4\ +\ Band\ 3} \quad (6)$$

In Landsat 8

$$NDVI = \frac{Band\ 5\ -\ Band\ 4}{Band\ 5\ +\ Band\ 4} \quad (7)$$

3. Result and Discussions

This study will calculate the progress of land surface temperature (LST) by using the Urban Index (UI) to identify the non-urban and urban area and Normalized Difference Vegetation Index (NDVI) to classify the non-vegetation and vegetation area by employing images taken from Landsat OLI 8 TRS in different time periods.

3.1. Normalized Difference Vegetation Index (NDVI)

The result of vegetation index analysis show that the vegetation area declines significantly in the last 4 years from 8335.76 hectare to 4865.11 hectare. The result of vegetation index shows that in 2015, Makassar had 0.63 value high vegetation index but in 2019 decreased to 0.56.

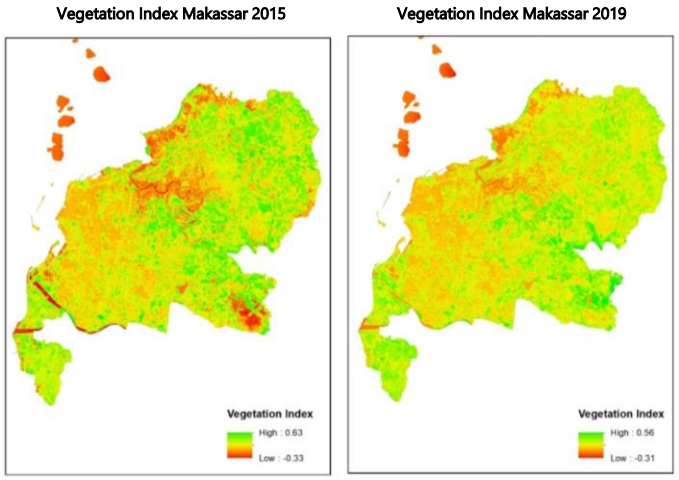

Figure 3. Normalized Difference Vegetation Index (NDVI) Makassar in 2015 – 2019.

3.2. Land Surface Temperature (LST)

The distribution of LST needs to be known in an area, so that it can be seen which areas have experienced an increase in surface temperature and can then be used in the land use and utilization planning process. This LST distribution can be done using remote sensing methods by utilizing satellite image data

The result of LST analysis shows that the highest temperature was 33 degree Celsius and the lowest was 18 degree Celsius in 2015. Meanwhile, 2019 shows that the highest temperature was 29 degree Celsius and the lowest was 17 degree Celsius. In addition, the Land Surface Temperature (LST) shows that the maximum temperature decreased from 33 degree Celsius in 2015 to 29 degree Celsius in 2019, however its distribution getting increased and covered wider area in 2019 than 2015.

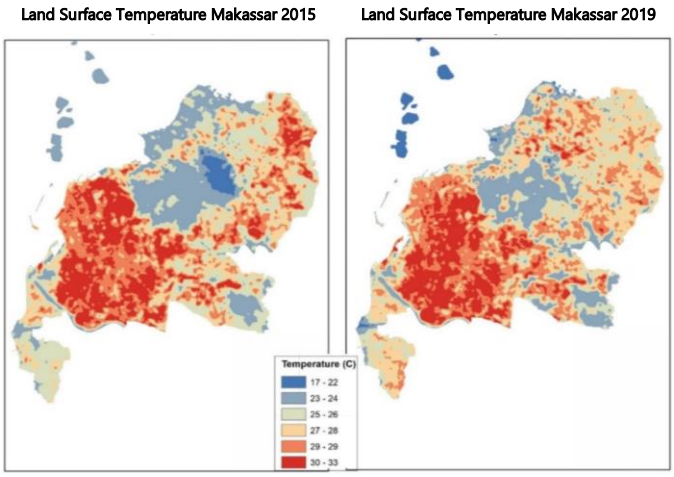

Figure 4. Land Surface Temperature (LST) Makassar in 2015 – 2019.

3.3. Correlation Analysis

The correlation analysis of NDVI and LST in 2015 and 2019 show that there is a significant relationship between low or no vegetation area (0 to 0.2 NDVI value) and maximum temperature (25 – 32 degree Celsius) as well as between high vegetation area (0.5 to 0.8 NDVI value) and minimum temperature (18 – 22 degree Celsius). The following figures show the correlation between vegetation index value and temperature index in two different time periods.

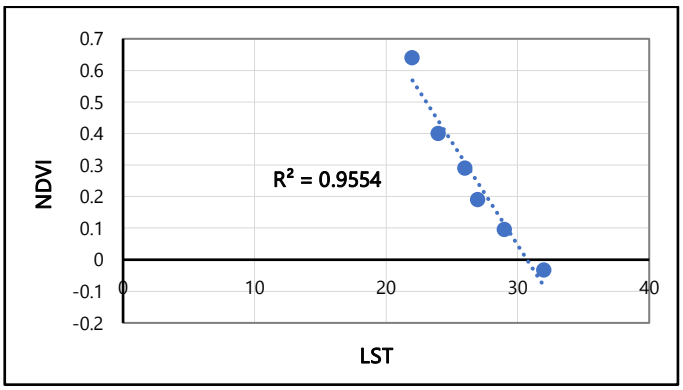

Figure 5. Correlation between NDVI and LST in 2015.

The most common measurement used to identify the density of plant growth over the entire globe is NDVI (Normalized Difference Vegetation Index). Calculations of NDVI for a given pixel result in a number ranges from minus one (-1) to plus one (+1). The lowest value of NDVI (-0.1 – below) indicated to the barren area of rock and sand (built up area). Moderate value (0.2 to 0.3) corresponds to grassland and shrub and high value of NDVI (0.6 to 0.8) represent to high vegetation density such as woodland and forest. Landsat 8 TIRS is employed because it could acquire LST temperature accurately. Even though the spatial resolution of TIRS is 100 m compared to 30 m Landsat 8 ETM+, it's two bands (10 and 11) is more accurate to estimate the land surface temperature than Landsat 8 ETM+ [31]. Furthermore, using 100 resolution is well enough for relatively homogeneous area and water consumption measurement [32].

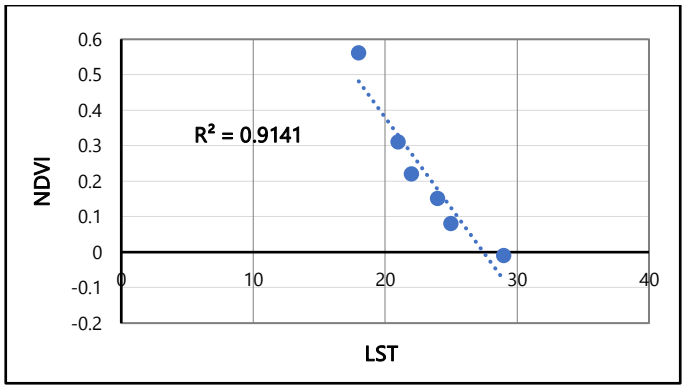

Figure 6. Correlation between NDVI and LST in 2019.

This research uses correlation analysis to assess the relationship between NDVI and LST in order to forecast the progress of land surface temperature in coming years. The result shows that the low or zero vegetation density (0 to 0.2) indicates high temperature (29 to 32 degree Celsius) while high vegetation density (0.5 to 0.6) associated with low temperature (18 – 22 degree Celsius). In 2015, it had the highest temperature at 32 degree Celsius while 2019 shows the maximum heat at 29 degree Celsius. However, the moderate and high temperature (26 – 29 degree Celsius) in 2017 expand and cover wider area than in 2013 as the area of vegetation declined and built-up area increased. Area of minimum temperature indicates that water body and the densification of plants can lower the temperature as they increase the evapotranspiration and maintain an increased heat meanwhile land use and land cover changes play significant role to affect the local climate and the density of land use can increase the temperature [33], [34].

Land Surface Temperature (LST) is a state that is controlled by the energy balance of the surface, atmosphere, thermal properties of the surface, and the subsurface media [35], [36]. LST is an important phenomenon in global climate change. As the content of greenhouse gases in the atmosphere increases, so will LSTs increase. This will result in melting glaciers and ice sheets and affect the vegetation of the area. The impact will be more in the monsoon area, because unpredictable rainfall will result in flooding and sea level rise [22]. LST can be defined as the average surface temperature of a surface which is represented in the scope of a pixel with a variety of different surface types [37]–[39]. Land Surface Temperature is one of the key parameters in various environmental studies in different disciplines, such as

geology, hydrology, ecology, oceanography, meteorology, climatology, and others [40]–[43]. LSTs control the flux of long-wave energy through the atmosphere. The size of LST depends on the conditions of other surface parameters, such as albedo, surface moisture and cover and vegetation conditions. Therefore, knowledge of the spatial distribution of LST and their temporal diversity is important for accurate modeling of flow between the surface and the atmosphere [44], [45]. The increase in LST also affects the climatic conditions of the monsoon area which causes unexpected rainfall [46].

Vegetation all over the earth's surface will be affected by this. Land use and land cover of an area can be used to estimate the value of land surface temperature. Natural and anthropogenic activities change the land use and cover of an area. It also affects the LST of the area. As a value of local climate change, LST is an important phenomenon to investigate. Therefore, many researchers have calculated LST using various algorithms and techniques [22]. So far, temperature data has been obtained using a thermometer that is installed on the ground to obtain the surface temperature value. Temperature can also be measured using a thermometer installed in the weather cage to get the surface air temperature. The temperature data is still local and local. Therefore, to obtain more regional temperature data, it is necessary to collect temperature data from several weather stations.

Collecting temperature data from multiple weather stations reduces the accuracy of the data. In addition, processing such data will take a lot of time if there is no mode of transmission or real time data transmission between weather stations. Therefore, collecting land surface temperature data will be much easier if you use remote sensing satellite data, among the advantages are the wide scope observed and areas that may be difficult to reach and the effectiveness of time [47]. Data or imagery from remote sensing satellites is processed with various corrections to get decent results. The satellite data must be processed using various appropriate formulas to be able to reduce the value of a good land surface temperature. Landsat 8 imagery can be processed with digital image processing to obtain information on land surface temperature. Information on land surface temperature can be derived from Landsat 8 through two channels, namely band 10 and band 11. The two channels need to be converted from the DN (Digital Number) value to the ToA (Top of Atmosphere) Radiance value. After both are converted into ToA Radiance values, then each is converted into a brightness temperature value in Kelvin [24].

4. Conclusion

Landsat 8 TIRS is used because it has high resolution thermal to derive LST temperature accurately to identify relatively homogeneous areas. The fact shows that the high and moderate vegetation density area associated with minimum temperature while low vegetation density area corresponds to maximum temperature.

Acknowledgments

This research is a collaboration between countries which aims to increase the global collaborative network of researchers. Thank you for the support provided by the university so that this article can be completed.

References

[1] M. L. Khandekar, T. S. Murty, and P. Chittibabu, "The global warming debate: A review of the state of science," *Pure Appl. Geophys.*, vol. 162, no. 8, pp. 1557–1586, 2005.

[2] P. K. Bhattacharjee, "Global warming impact on the earth," *Int. J. Environ. Sci. Dev.*, vol. 1, no. 3, p. 219, 2010.

[3] M. Bokaie, M. K. Zarkesh, P. D. Arasteh, and A. Hosseini, "Assessment of urban heat island based on the relationship between land surface temperature and land use/land cover in Tehran," *Sustain. Cities Soc.*, vol. 23, pp. 94–104, 2016.

[4] K. S. Kumar, P. U. Bhaskar, and K. Padmakumari, "Estimation of land surface temperature to study urban heat island effect using LANDSAT ETM+ image," *Int. J. Eng. Sci. Technol.*, vol. 4, no. 2, pp. 771–778, 2012.

[5] R. C. Estoque, Y. Murayama, and S. W. Myint, "Effects of landscape composition and pattern on land surface temperature: An urban heat island study in the megacities of Southeast Asia," *Sci. Total Environ.*, vol. 577, pp. 349–359, 2017.

[6] Q. Weng, D. Lu, and J. Schubring, "Estimation of land surface temperature–vegetation abundance relationship for urban heat island studies," *Remote Sens. Environ.*, vol. 89, no. 4, pp. 467–483, 2004.

[7] C. P. Morice *et al.*, "An updated assessment of near-surface temperature change from 1850: the HadCRUT5 dataset," *J. Geophys. Res. Atmos.*, p. e2019JD032361, 2020.

[8] M. I. Ali, G. D. Dirawan, A. H. Hasim, and M. R. Abidin, "Detection of Changes in Surface Water Bodies Urban Area with NDWI and MNDWI Methods," *Int. J. Adv. Sci. Eng. Inf. Technol.*, vol. 9, no. 3, pp. 946–951, 2019.

[9] M. I. Ali, A. H. Hasim, and M. R. Abidin, "Monitoring the Built-up Area Transformation Using Urban Index and Normalized Difference Built-up Index Analysis," *Int. J. Eng. Trans. B Appl.*, vol. 32, no. 5, pp. 647–653, 2019.

[10] S. Sloan *et al.*, "Infrastructure development and contested forest governance threaten the Leuser Ecosystem, Indonesia," *Land use policy*, vol. 77, pp. 298–309, 2018.

[11] K. Tzoulas *et al.*, "Promoting ecosystem and human health in urban areas using Green Infrastructure: A literature review," *Landsc. Urban Plan.*, vol. 81, no. 3, pp. 167–178, 2007.

[12] F. Ascensão *et al.*, "Environmental challenges for the Belt and Road Initiative," *Nat. Sustain.*, vol. 1, no. 5, pp. 206–209, 2018.

[13] J. A. Patz, S. H. Olson, C. K. Uejio, and H. K. Gibbs, "Disease emergence from global climate and land use change," *Med. Clin. North Am.*, vol. 92, no. 6, pp. 1473–1491, 2008.

[14] Z. Wan, P. Wang, and X. Li, "Using MODIS land surface temperature and normalized difference vegetation index products for monitoring drought in the southern Great Plains, USA," *Int. J. Remote Sens.*, vol. 25, no. 1, pp. 61–72, 2004.

[15] F. S. Chapin *et al.*, "Role of land-surface changes in Arctic summer warming," *Science (80-.).*, vol. 310, no. 5748, pp. 657–660, 2005.

[16] Y. Zhang, A. Harris, and H. Balzter, "Characterizing fractional vegetation cover and land surface temperature based on sub-pixel fractional impervious surfaces from Landsat TM/ETM+," *Int. J. Remote Sens.*, vol. 36, no. 16, pp. 4213–4232, 2015.

[17] Z. Zhang, M. Ji, J. Shu, Z. Deng, and Y. Wu, "Surface urban heat island in Shanghai, China: Examining the relationship between land surface temperature and impervious surface fractions derived from Landsat ETM+ imagery," *Int. Arch. Photogramm. Remote Sens. Spat. Inf. Sci*, vol. 37, pp. 601–606, 2008.

[18] H. Tran, D. Uchihama, S. Ochi, and Y. Yasuoka, "Assessment with satellite data of the urban heat island effects in Asian mega cities," *Int. J. Appl. Earth Obs. Geoinf.*, vol. 8, no. 1, pp. 34–48, 2006.

[19] T. N. Carlson, J. A. Augustine, and F. E. Boland, "Potential application of satellite temperature measurements in the analysis of land use over urban areas," *Bull. Am. Meteorol. Soc.*, pp. 1301–1303, 1977.

[20] R. Maru, M. R. Abidin, A. Arfan, S. Nyompa, U. Uca, and S. Hasja, "Mapping of Protected Forests and Cultivated Area in North Luwu South Sulawesi, Indonesia," *Asian J. Aplied Sci.*, 2016.

[21] A. Arfan *et al.*, "Production and decomposition rate of litterfall Rhizophora mucronata," *Environ. Int. J. by Thai Soc. High. Educ. Institutes Environ.*, vol. 11, no. 1, pp. 1–242, 2018.

[22] A. Rajeshwari and N. D. Mani, "Estimation of land surface temperature of Dindigul district using Landsat 8 data," *Int. J. Res. Eng. Technol.*, vol. 3, no. 5, pp. 122–126, 2014.

[23] V. Otero, C. Mosier, and D. Neuberger, "Thermal Infrared Sensor (TIRS) Instrument Thermal Subsystem Design and Lessons Learned," in *43rd International Conference on Environmental Systems*, 2013, p. 3445.

[24] U.S. Geological Survey, "Mineral Commodity Summaries," Reston, VA, 2014. doi: 10.3133/70100414.

[25] R. Maru and S. Ahmad, "The relationship between land use changes and the urban heat island phenomenon in Jakarta, Indonesia," *Adv. Sci. Lett.*, vol. 21, no. 2, pp. 150–152, 2015.

[26] A. Rifani, E. A. Saputro, I. Invanni, and R. Maru, "Study of Land Surface Temperature Using Remote Sensing Satellite Imagery in makassar, Sout Sulawesi," in *Proceeding of 9th InternationalGraduate Students and Scholars' Conference in Indonesia (IGSSCI), The 9th In*, 2017, pp. 179–190.

[27] R. Maru *et al.*, "Analysis of The Heat Island Phenomenon in Makassar, South Sulawesi, Indonesia," *Am. J. Appl. Sci.*, vol. 12, no. 9, 2015.

[28] BPS-Statistics of Makassar, *Makassar in Figures*. Makassar: BPS-Statistics of Makassar, 2018.

[29] Product Guide, "Landsat Surface Reflectance-Derived Spectral Indices; 3.6 Version," *Dep. Inter. US Geol. Surv. Reston, VA, USA*, 2017.

[30] N. Landsat, "Science Data Users Handbook," *Availabe online http//landsathandbook. gsfc. nasa. gov/inst_cal/prog_sect8_2. html (7)(accessed 11 March 2011)*, 7AD.

[31] O. Rozenstein, Z. Qin, Y. Derimian, and A. Karnieli, "Derivation of land surface temperature for Landsat-8 TIRS using a split window algorithm," *Sensors*, vol. 14, no. 4, pp. 5768–5780, 2014.

[32] J. R. Irons, J. L. Dwyer, and J. A. Barsi, "The next Landsat satellite: The Landsat data continuity mission," *Remote Sens. Environ.*, vol. 122, pp. 11–21, 2012.

[33] O. Orhan, S. Ekercin, and F. Dadaser-Celik, "Use of landsat land surface temperature and vegetation indices for monitoring drought in the Salt Lake Basin Area, Turkey," *Sci. World J.*, vol. 2014, 2014.

[34] J. P. Joshi and B. Bhatt, "Estimating temporal land surface temperature using remote sensing: A study of Vadodara urban area, Gujarat," *Int. J. Geol. Earth Environ. Sci.*, vol. 2, no. 1, pp. 123–130, 2012.

[35] F. Becker and Z.-L. Li, "Temperature-independent spectral indices in thermal infrared bands," *Remote Sens. Environ.*, vol. 32, no. 1, pp. 17–33, 1990.

[36] F. Becker and Z.-L. Li, "Towards a local split window method over land surfaces," *Remote Sens.*, vol. 11, no. 3, pp. 369–393, 1990.

[37] Y. Chen *et al.*, "Improving land surface temperature modeling for dry land of China," *J. Geophys. Res. Atmos.*, vol. 116, no. D20, 2011.

[38] Z. Wan and J. Dozier, "A generalized split-window algorithm for retrieving land-surface temperature from space," *IEEE Trans. Geosci. Remote Sens.*, vol. 34, no. 4, pp. 892–905, 1996.

[39] A. Benali, A. C. Carvalho, J. P. Nunes, N. Carvalhais, and A. Santos, "Estimating air surface temperature in Portugal using MODIS LST data," *Remote Sens. Environ.*, vol. 124, pp. 108–121, 2012.

[40] D. Skoković *et al.*, "Calibration and Validation of land surface temperature for Landsat8-TIRS sensor," *L. Prod. Valid. Evol.*, 2014.

[41] J. A. Sobrino *et al.*, "Land surface emissivity retrieval from different VNIR and TIR sensors," *IEEE Trans. Geosci. Remote Sens.*, vol. 46, no. 2, pp. 316–327, 2008.

[42] J. C. Jiménez-Muñoz, J. Cristóbal, J. A. Sobrino, G. Sòria, M. Ninyerola, and X. Pons, "Revision of the single-channel algorithm for land surface temperature retrieval from Landsat thermal-infrared data," *IEEE Trans. Geosci. Remote Sens.*, vol. 47, no. 1, pp. 339–349, 2008.

[43] J.-C. Jiménez-Muñoz and J. A. Sobrino, "Split-window coefficients for land surface temperature retrieval from low-resolution thermal infrared sensors," *IEEE Geosci. Remote Sens. Lett.*, vol. 5, no. 4, pp. 806–809, 2008.

[44] G. C. Hulley, D. Ghent, F. M. Göttsche, P. C. Guillevic, D. J. Mildrexler, and C. Coll, "Land Surface Temperature," in

Taking the Temperature of the Earth, Elsevier, 2019, pp. 57–127.

[45] J. D. Kalma, T. R. McVicar, and M. F. McCabe, "Estimating land surface evaporation: A review of methods using remotely sensed surface temperature data," *Surv. Geophys.*, vol. 29, no. 4–5, pp. 421–469, 2008.

[46] Y. Zhang, I. O. A. Odeh, and C. Han, "Bi-temporal characterization of land surface temperature in relation to impervious surface area, NDVI and NDBI, using a sub-pixel image analysis," *Int. J. Appl. Earth Obs. Geoinf.*, vol. 11, no. 4, pp. 256–264, 2009.

[47] D. A. Quattrochi and J. C. Luvall, *Thermal remote sensing in land surface processing*. CRC Press, 2004.